



Fire whirls behind an L-shaped wall in a crossflow

Tomomi Sasaki, Moe Igari, Kazunori Kuwana*

Department of Chemistry and Chemical Engineering, Yamagata University, 4-3-16 Jonan, Yonezawa, Yamagata 992-8510, Japan



ARTICLE INFO

Article history:

Received 5 February 2018

Revised 23 June 2018

Accepted 28 June 2018

Keywords:

Fire whirl

Crossflow

Particle image velocimetry (PIV)

Flame height

Scaling law

Froude number

ABSTRACT

This paper studies fire whirls formed behind an L-shaped wall in a crossflow. Wind-tunnel experiments at various crossflow velocities were conducted, and it was found that there was a narrow range of crossflow velocity that led to the formation of an intense and stable fire whirl, i.e., the existence of a critical wind velocity. Scaling analysis and computational fluid dynamics (CFD) calculations of different scales suggested that the Froude number is the governing parameter of the phenomenon; the critical wind velocity is therefore roughly proportional to the square root of the fire size. Particle image velocimetry (PIV) measurements showed that the rotational velocity component was reduced near the bottom floor, which then induced a fast radial inflow toward the axis in the vicinity of the floor. This radial inflow pushes the flame toward the fuel surface, enhancing heat transfer between flame and fuel and thereby leading to the formation of an intense fire whirl. The inflow velocity was much slower when the crossflow velocity was outside the critical range. Finally, it was demonstrated that the formation of an intense fire whirl could be prevented by blocking the near-floor flow using an obstacle.

© 2018 The Combustion Institute. Published by Elsevier Inc. All rights reserved.

1. Introduction

Fire whirls, when they occur during an urban or wildland fire, can intensify its burning rate and make sudden and unpredictable changes of the direction in which the fire spreads. Both effects make firefighting efforts dangerous and difficult, as can be seen in the past literature where casualties were reported [1–3]. It is crucial to understand the mechanism of fire whirls to develop an effective firefighting strategy and a method that can effectively cope with the transient nature of fire behavior.

A number of fire-whirl studies were conducted using rotating or fixed-frame devices. Early investigators [4–6] developed simple models to predict the average core properties of a fire whirl along its axis. Later papers reported numerical simulations of fire whirls [7–11], revealing the detailed structures of interactions between fires and vortices. The mechanism of flame-height increase has been often addressed [10–14], and recent studies [15,16] suggested that the intensity of a fire whirl is enhanced by a near-ground flow toward the axis that tends to increase the heat feedback to the fuel and hence the burning rate. Tohidi et al. [17] recently published a review article on fire whirls.

Urban and wildland fire whirls are, however, generated by interactions between fires and crossflows [1–3]. Although several researchers successfully reproduced fire whirls using wind tunnels

[2,3,18–21], their detailed structures, in particular, flow structures around them are not yet clearly understood because of the unstable and moving nature of fire whirls generated by crossflows as reported in the previous studies [18–21]. To overcome the difficulty, this study uses an L-shaped wall in a crossflow; by placing a fire source in the recirculation region behind the wall, a stable fire whirl can be formed above the fire source, enabling detailed flow measurements. Computational fluid dynamics (CFD) simulations were additionally conducted to provide information that was difficult to obtain experimentally.

There are two major objectives in this study. The first is to examine whether a near-ground flow toward the axis is necessary to generate a stable fire whirl in a crossflow similarly to fire whirls created by rotating or fixed-frame devices. The second objective is to understand the scaling law of fire whirls in crossflows so that the insights obtained by wind-tunnel experiments can be applied to large-scale fires with a particular focus on the dynamic similarity (i.e., similarity of flow structures) between fire whirls of different scales. Based on obtained results, a preventive measure is proposed that can reduce the intensity of fire whirl.

2. Experimental and numerical methods

2.1. Experimental method

Figure 1(a) shows a schematic diagram of the present experiment, where a methanol pool fire of 6 cm × 6 cm was placed behind an L-shaped wall of 9 cm × 18 cm in a crossflow of a

* Corresponding author.

E-mail address: kuwana@yz.yamagata-u.ac.jp (K. Kuwana).

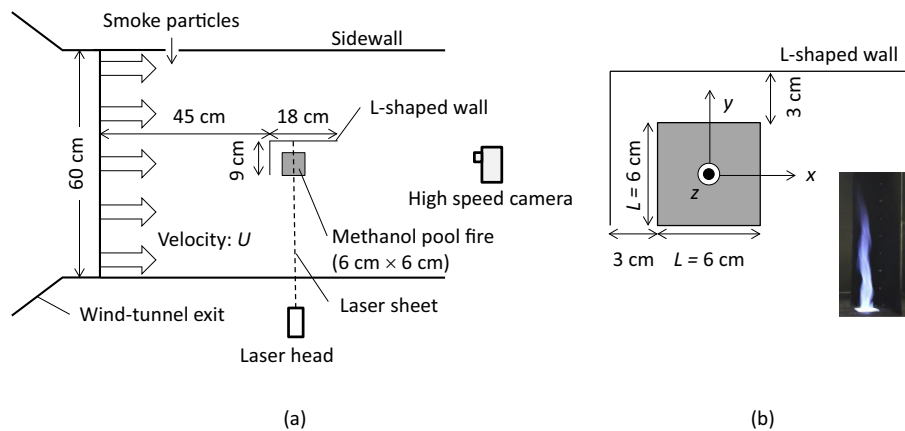


Fig. 1. Experimental setup to generate a fire whirl behind an L-shaped wall.

specified velocity provided by a wind tunnel. The center of the pool is equidistant from the sidewalls. The location of the L-shaped wall was 45 cm away from the wind-tunnel exit. Methanol was used for the following two reasons: (1) its weak emission of light enables accurate particle image velocimetry (PIV) measurement of near-flame velocity distributions, and (2) experimental data can be compared with CFD predictions that neglect soot formation. The size of the wind-tunnel exit is 60 cm × 60 cm, and the height of the L-shaped wall is also 60 cm. A typical fire whirl created by this setup is shown in the inset of Fig. 1(b), which also shows the coordinates used throughout this study. The x - y plane is horizontal, while the z axis denotes the height from the bottom floor. The origin of the coordinates is at the center of the fuel surface.

The average flame height under a crossflow velocity, varied from 0.1 to 0.8 m/s, was obtained by image analysis. Methanol of 15 g was burned, and the evolution of flame was recorded from the downstream side by a digital camera at a time interval of 1/3 s. Each image was converted into a binary image, from which the instantaneous flame height was determined. The flame tip was sometimes separated from the continuous flame region. The height of the continuous flame region was recorded as the flame height in such a case.

Velocity distributions around a flame were measured by a PIV method. The configuration shown in Fig. 1(a) illustrates the PIV system used to measure the flow field on the y - z plane. A smoke generator placed in an upstream location provided fine smoke particles (average diameter, 10 μm) by vaporizing a glycol solution through a hole of 53 mm in diameter on the sidewall. The particles were illuminated by a 450 mW Nd:YVO₄ laser sheet. A high speed camera with a bandpass filter recorded images of illuminated smoke particles at 1000 frames per second from the downstream side. For measuring velocity distributions on the x - y plane, on the other hand, a horizontal laser sheet at a given height was applied while recording high speed images from above.

2.2. Numerical model

CFD calculations were conducted using ANSYS Fluent for the configuration shown in Fig. 1. The large eddy simulation (LES) turbulence model was used, and the subgrid-scale eddy viscosity was dynamically computed by accounting for the transport of the subgrid-scale turbulence kinetic energy. The mixture fraction model was used with the assumptions of chemical equilibrium among 18 species (fuel, O₂, CO₂, H₂O, CO, H₂, H, OH, CH₂O, CH₄, HCOOH, HO₂, O, HONO, H₂O₂, CHO, HCO, and N₂) and the beta function for the probability density function (PDF), together with a user-defined subroutine to compute the evaporation of methanol

at its boiling point according to the heat flux to the liquid surface as [11]

$$u_z = \frac{k_g}{\rho_g H_{\text{vap}}} \frac{\partial T}{\partial z} \text{ at } z = 0 \text{ and } |x|, |y| \leq 3 \text{ cm} \quad (1)$$

where u_z is the z -velocity of fuel vapor, k_g the gas-phase thermal conductivity, ρ_g the gas-phase density, and H_{vap} the heat of evaporation.

The size of the computational domain, 36 cm in $x \times 30$ cm in $y \times 50$ cm in z , is smaller than that of the actual test section of the experiment to reduce the computational time. An inlet boundary condition with a constant crossflow velocity was imposed at $x = -15$ cm. Periodic boundary conditions were adopted in the transverse direction to eliminate the wall effects in the computation. Since the size of the computational domain is smaller than that of the experimental test section, wall effects would be more enhanced than the experiment if wall boundary conditions were used. It was confirmed that the predicted flows near the periodic boundaries were nearly parallel to them. As to the height of the computational domain, it is more than two times as large as the maximal flame height observed experimentally, so that the effects of the top boundary on flame height and near-ground flow are expected to be negligible.

The size of computational cell on the x - y plane within the L-shaped wall was uniform and 5 mm, while the unevenly distributed cells were used outside the L-shaped wall with the coarsest cell (10 mm) on the periodic boundaries. Unevenly distributed computational cells were also used in the z direction with the finest cell (0.5 mm) on the bottom surface and the coarsest cell (20 mm) on the top boundary at $z = 50$ cm. A calculation using half-size cells (1/8 in cell volume) was conducted for a test of cell-size dependence. The difference in the average flame height at $U = 0.4$ m/s was less than 5%.

Calculations for 12 different crossflow velocities ranging from 0.1 to 1 m/s were conducted. The simulated period of time was 30 s under each condition, and the last 10 s was used for obtaining a time-averaged solution. In addition to the 12 baseline computations, calculations for the double-scale geometry, in which every geometrical configuration including the domain size was enlarged two times in all the x , y , and z directions, were also conducted to study the scale effect of the phenomenon. In the double-scale case, the last 15 s was used for obtaining a time-averaged solution. Note that the double-scale calculations used as fine computational cells as the baseline cases. Furthermore, calculations with varied values of the acceleration of gravity, g , were conducted to further examine the scaling law.

Download English Version:

<https://daneshyari.com/en/article/11000295>

Download Persian Version:

<https://daneshyari.com/article/11000295>

[Daneshyari.com](https://daneshyari.com)